Theoretical Study of the Cage Water Hexamer Structure

Jonathon K. Gregory

Department of Chemistry, University of Cambridge, Cambridge, CB2 1EW, U.K.

David C. Clary*

Department of Chemistry, University College London, London, WC1H 0AJ, U.K.

Received: January 31, 1997; In Final Form: March 25, 1997[⊗]

We present a theoretical examination of the structures and dynamics of a "cage" form of the water hexamer which has recently been observed experimentally. A thorough examination with one of the best many-body water potentials is used to characterize minima, transition states, and reaction paths. All of the rearrangements characterized have pathways similar to those already seen for the water dimer and trimer. The accuracy of this empirical potential is assessed by comparison with MP2 optimizations, and good agreement in terms of the topology of the intermolecular potential energy surface is seen. Quantum simulation using the diffusion quantum Monte Carlo method is used to show that the ground state wave function is dominated by one minimum in the water hexamer potential.

1. Introduction

Research on small water clusters is of fundamental importance in moving toward an understanding of bulk water. Such studies provide a bridge between the water dimer, the structure of which is known experimentally[1] and has also been characterized quite well theoretically,[2] and the condensed phase. In working toward a complete model of the liquid, it is important to gain a detailed understanding of the nonpairwise additive interactions which play a significant role in determining the nature of the intermolecular forces between water molecules. Recent experimental advances resulting from the advent of far-infrared vibration−rotation tunneling (FIR-VRT) spectroscopy,[3−5] high-level *ab initio* electronic structure calculations,[6−9] and vibrational diffusion quantum Monte Carlo (DQMC) studies[10−14] have all been important in probing the structures and dynamics of small water clusters.

The minimum energy structures of the water trimer,[15−19] tetramer,[20−25] and pentamer[6,7,25−27] are known to be cyclic and have all been assigned as such in experiments.[16,21,22,26] The heptamer, octamer, and larger clusters are expected to have three-dimensional geometries[20,28] and, consequently, the water hexamer is seen to represent a crossover point and is also the smallest water cluster for which the most stable geometry is not well characterized. However, a recent study combining FIR-VRT spectroscopy and DQMC simulations has identified a three-dimensional cage form of the water hexamer (Figure 1). Given the low temperatures (6 K) of the supersonic jets used in FIR-VRT experiments,[29] it is likely that this cage structure is indeed the most stable form of the water hexamer.

Before the experimental observation of the cage water hexamer,[30] all theoretical studies had been concerned with the relative stability of a number of different minima on the potential energy surface.[8,31−39] However, given that the cage structure has now been observed experimentally, it is appropriate to use well-established theoretical methods to understand more fully its dynamics. The background to the methods used for this is given in section 2. It is not clear whether the experimentally observed structure corresponds to a single minimum on the IPES or is a superposition of more than one structure. We therefore employ an exhaustive search for minima, transition states, and corresponding reaction paths. One of the best water potentials is used together with *ab initio* optimizations at the MP2 level of theory, all of which are reported in section 3. It is shown that there are a number of minima very similar to that shown in Figure 1 and that transition states exist to interconvert them. A discussion of the rotational constants of the various minima is given in section 4 and compared to the experimental values. Finally, in section 5, we perform quantum simulations to obtain the ground state wave function and to verify the structure or structures to which this corresponds. Our conclusions are presented in section 6.

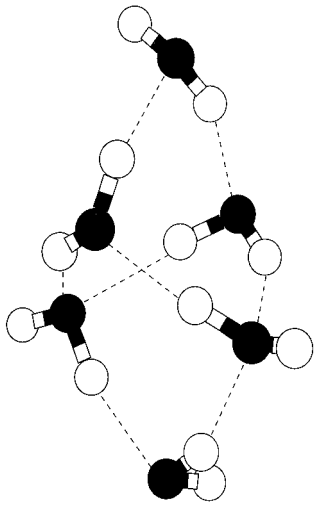

Figure 1. A cage structure of the water hexamer.

2. Theory

A. Study of IPES. The intermolecular potential energy surface (IPES) is based on the pairwise water dimer potential of Millot and Stone[40] which is known as ASP-W2.[41] This contains many-body forces in the form of an iterated induction energy. Although it is not expected to be as accurate as the best *ab initio* calculations, the use of an analytical potential facilitates a rigorous study of the region of the water hexamer IPES in which we are interested.

* To whom correspondence should be addressed.

[⊗] Abstract published in *Advance ACS Abstracts,* July 1, 1997.

S1089-5639(97)00387-3 CCC: $14.00

ORIENT 3[42−44] is a program which employs a distributed multipole analysis[45,46] to calculate intermolecular interaction energies. The first and second derivatives of these energies, with respect to rigid body coordinates, may be obtained[47] and eigenvector-following[48] used to explore the topology of the IPES. In particular, the calculation of transition states and reaction paths, as well as minima, is particularly useful. The ASP-W2 IPES will be used in conjunction with ORIENT 3.

In ref 30, quantum simulation of the ground vibrational states of the cage water hexamer yielded rotational constants of $A =$ 2136 MHz, $B =$ 1096 MHz, and $C =$ 1043 MHz, within 1%, 3%, and 2%, respectively, of the experimental numbers (given in the same paper). However, this agreement does not show whether the experiment is showing a vibrationally averaged version of one minima, such as shown in Figure 1, or if other structures are important. In order to address this question, new geometry optimizations are carried out with the ORIENT 3/ASP-W2 description of the system. The starting structures are displaced by varying amounts from the cage structure shown in Figure 1. We searched first for minima and then for transition states, completing a total of 8000 optimizations. Over 100 different minima are characterized this way and the rotational constants of each were examined. Only structures which give rotational constants within 10% of the theoretical ground state values quoted above are considered. A large number of transition states also were located and the corresponding reaction paths calculated. Only if both minima have rotational constants within 10% of the theoretical ground state results are the reaction path and transition state examined.

B. *Ab Initio* Calculations. In order to access the accuracy of the ASP-W2 surface, *ab initio* geometry optimizations from ASP-W2 minima and transition states were performed. All *ab initio* calculations used the Cambridge Analytical Derivatives Package (CADPAC)[49] and second-order Møller−Plesset perturbation theory (MP2).[50] Double-zeta plus polarization (DZP)[51] and the more flexible 6-31+G[2d,1p] basis set described by Jordan and co-workers were used.[9,52] The DZP basis set is not ideal for water clusters but was the largest basis set that could realistically be used for geometry optimizations on all the ASP-W2 stationary points. We expect that the structures obtained at this level of theory should be fairly accurate but that the interaction energies may be less so since the electrical properties with the DZP basis set are likely to be underestimated. The 6-31+G[2d,1p] basis set, which gives results similar to those of the large aug-cc-VDZ basis set[53] for the water monomer and dimer, should provide better estimates of energies and will be used for some points as a comparison with the DZP/MP2 values.

The *ab initio* calculations used ASP-W2 geometries as starting points. These structures were generally seen to be fairly good guesses since the initial root-mean-square gradients for the geometry optimizations were generally quite small ($\sim 10^{-3}$ hartree a_0^{-1}). The optimizations were terminated when the maximum step length was less than 10^{-5} au; this is quite a tight convergence criterion since the potential energy surfaces involved are relatively flat. A normal-mode analysis was performed to identify minima (no imaginary frequencies) and transition state (one imaginary frequency).

C. DQMC Calculations. The quantum simulation of the vibrational ground state of the cage hexamer was performed using diffusion Monte Carlo (DQMC). DQMC has been used as an algorithm to solve electronic structure problems[54,55] and the method was applied to vibrational problems by Watts and co-workers.[56] There have been many applications of this method to vibrational problems in the last decade (e.g. see refs 57−61). We[10−12,30,14,62] and others[57,58,63,64] have applied the DQMC method to water clusters.

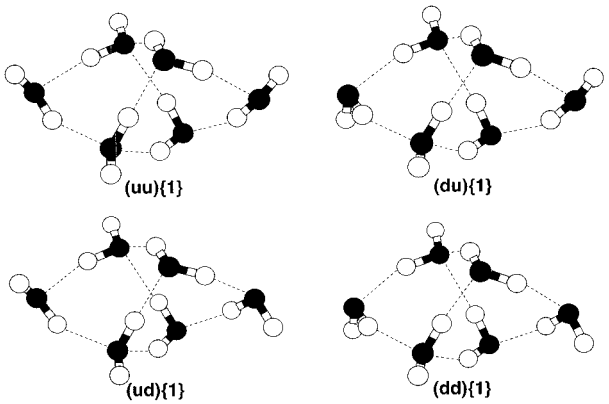

Figure 2. Four distinct but nearly isoenergetic cage structures for the water hexamer, known as subset {1}.

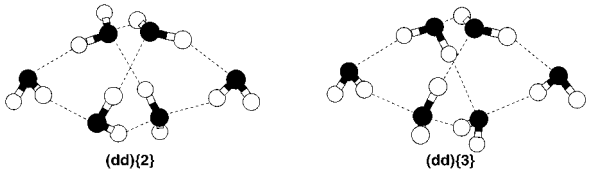

Figure 3. Structures representing the other two subsets of four cage structures for the water hexamer, known as subsets {2} and {3}. Shown are the lowest energy structures for the (uu), (du), (ud), and (dd) forms.

Since the ASP-W2 describes only intermolecular degrees of freedom, we use the rigid body DQMC formalism as first described by Buch.[60] This approach, known as RBDMC, has been shown to give good agreement with the fully dimensional calculations for the water dimer[62,65] and has been extended to larger water clusters,[10−14,30] including the hexamer.[13,14,30] The precise formalism and computational details have been described by us previously.[10]

In the RBDMC simulation, a population of 3000 replicas was subject to an equilibrium stage of 5000 steps of 50 au and a propagation stage of 25 000 steps of 20 au, over which properties were averaged. Descendant weighting[66] was used to estimate rotational constants, and wave functions were constructed as histograms over the coordinate in question.

3. Results

A. Minima. There are four almost degenerate versions of the cage structure shown in Figure 1 which differ only in the position of two unbound hydrogens on the far left and right. These four additional structures are shown in Figure 2. They are labeled according to the up and down nature of the free hydrogens, by which the four minima differ. The energetic ordering is (uu) < (du) < (ud) < (dd) for the ASP-W2 surface, and the relative energies of the latter three structures are +46, +66, and +82 cm^{-1}. The DZP/MP2 ordering is (du) < (uu) < (dd) < (ud) where the latter three have relative energies of +9, +39, and +78 cm^{-1}. The 6-31+G[2d,1p]/MP2 ordering is different again, du < dd < uu < ud with the relative energies of the latter three structures being +41, +51, and +110 cm^{-1}. Although the ordering of the structures is different in all three cases, all methods are in reasonable agreement in terms of the close proximity in energy of the four cage structures.

There are two more sets of four cagelike structures, and the ASP-W2 (ud) conformations of each are shown in Figure 3. These sets of four structures will be referred to by {2} for those on the left and {3} for those on the right so that the structures shown would be labeled (dd){2} and (dd){3} as shown. The

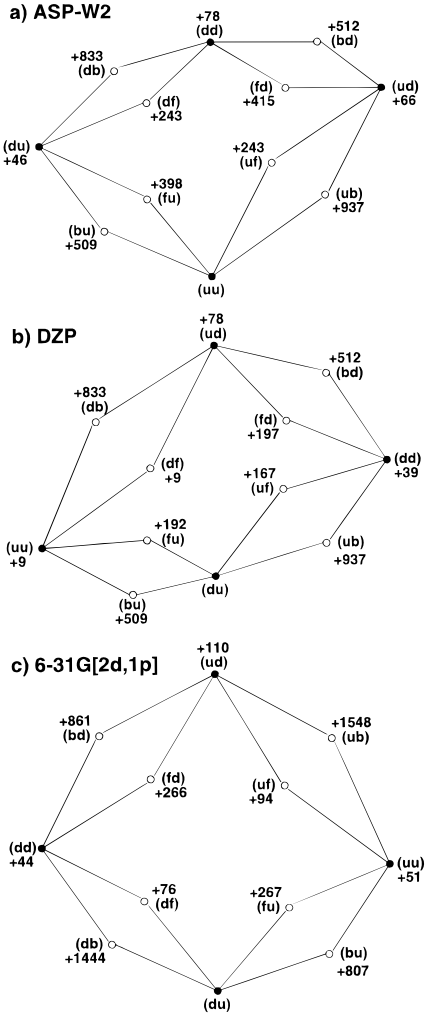

Figure 4. Diagrams showing the arrangement of four minima (filled circles) and eight transition states (circles) for the structures in subset {1} shown for the empirical potential and the two *ab initio* surfaces.

structures corresponding to subsets {2} are on average 407 cm^{-1} (ASP-W2) and 597 cm^{-1} (DZP/MP2) higher than the lowest four structures, referred to as {1}. The corresponding average between subsets {1} and {3} is 482 cm^{-1} (ASP-W2) and 710 cm^{-1} (DZP/MP2).

The {2} structures have a relative ordering of (ud) < (uu) < (dd) < (du) with relative energies of +148, +219, and +385 cm^{-1} (ASP-W2) and +185, +275, and +481 cm^{-1} (DZP/MP2). For the {3} structures, the ordering of (ud) < (dd) < (uu) < (du) gives relative energies of +206, +224, +440 cm^{-1} (ASP-W2) and the DZP/MP2 relative energies are 257, 261, and 556 cm^{-1} from a different ordering of (ud) < (uu) < (dd) < (du). The {2} and {3} subsets are not only higher in energy than those in Figure 2 but are also spaced farther apart.

B. Transition States. Just as important a question as the relative stabilities of the four cages is whether, and if so how

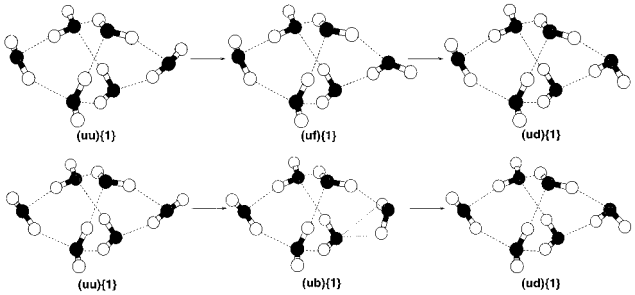

Figure 5. One each of the four single flip and bifurcation rearrangements which link the (uu), (du), (ud), and (dd) structures in subset {1}.

trivially, they may be interconverted. Eight transition states exist on the ASP-W2 IPES to facilitate rearrangements of each of the four structures in each subset. For each set of minima, there are four single flips and four bifurcations by which the four are linked. Each individual minimum is linked directly by a transition state to only two of the other three minima. Figure 4 shows this for the ASP-W2, DZP/MP2, and 6-31G[2d,1p]/MP2 surfaces. The four minima are depicted by filled circles, and the three numbers represent the relative energy with respect to the lowest energy conformation. Open circles show the eight transition states with numbers for the barrier heights with respect to the lowest of the two minima in question.

An example of each type of rearrangement is illustrated in Figure 5 for two of the structures in Figure 2. The transition states are labeled where f and b indicate that a monomer is in the process of undergoing a flip or bifurcation, respectively. The two dotted (rather than dashed) lines for the (ub) transitions state indicate the bifurcation; these hydrogen bond distances are 2.52 and 2.60 Å, compared to the original distance of 2.11 Å. Four second order saddle points connect the (uu)/(dd) and (ud)/(du) structures, which cannot be interconverted by only one flip or bifurcation.

In Table 1 are shown relative energies for the four minima and eight transition states for the first subset of structures. The difference between the two minima is given by ΔE_{min} while the difference between the corresponding transition state and the lower of the two minima is given by ΔE_{ts}. The bifurcation barriers are always above those for the corresponding flip which is not surprising since they involve a hydrogen bond exchange. The relative energies of the four minima and eight transition states are shown in Tables 2 and 3 for subsets {2} and {3}, respectively. As for subset {1}, the ASP-W2 barriers are generally lower than the DZP/MP2 ones for the single flip tunneling and vice versa for the bifurcation tunneling.

Since the four cage structures in Figure 2 are so close in energy and since the relatively facile rearrangements linking them have fairly low energy transition states, it is a possibility that the experimentally observed cage structure is in fact a superposition of more than one of these structures. The other two subsets of four structures lie sufficiently low in energy that

TABLE 1: Details of the Eight Rearrangements Which Interconvert the Four Minima in Subset {1}[a]

					single flip				bifurcation			
min1	min2	ΔE_{min}^{asp}	$\Delta E_{min}^{mp2\ b}$	$\Delta E_{min}^{mp2\ c}$	TS	ΔE_{ts1}^{asp}	$\Delta E_{ts1}^{mp2\ b}$	$\Delta E_{ts1}^{mp2\ c}$	TS	ΔE_{ts2}^{asp}	$\Delta E_{ts2}^{mp2\ b}$	$\Delta E_{ts1}^{mp2\ c}$
(uu)	(ud)	+66	+69	+59	(uf)	+243	+167	+94	(ub)	+937	+1548	+1597
(ud)	(dd)	+16	−39	−66	(fd)	+415	+197	+266	(bd)	+512	+861	+892
(dd)	(du)	−36	−39	−44	(df)	+243	+9	+76	(db)	+833	+1444	+1502
(du)	(uu)	−46	+9	+51	(fu)	+398	+192	+267	(bu)	+509	+807	+798

[a] The labels min1 and min2 refer to the two minima with ΔE_{min} giving the energy difference between them, E(min2) − E(min1), for the ASP and MP2 calculations. The four single flip and bifurcation transition states are given in the same way with ΔE_{ts1} and ΔE_{ts2} representing the barrier heights with respect to the lowest of min1 or min2. All units are in wavenumbers. [b] With DZP basis set. [c] With 6-31+G[2d,1p] basis set.

TABLE 2: Details of the Eight Rearrangements Which Interconvert the Four Minima in Subset {2}[a]

				single flip			bifurcation		
min1	min2	ΔE_{min}^{asp}	$\Delta E_{min}^{mp2\ b}$	TS	ΔE_{ts1}^{asp}	$\Delta E_{ts1}^{mp2\ b}$	TS	ΔE_{ts2}^{asp}	$\Delta E_{ts2}^{mp2\ b}$
(uu){2}	(ud){2}	−148	−185	(uf)	+327	+167	(ub)	+601	+807
(ud){2}	(dd){2}	+219	+275	(fd)	+475	+395	(bd)	+912	+1444
(dd){2}	(du){2}	+166	+206	(df)	+343	+160	(db)	+626	+861
(du){2}	(uu){2}	−237	−296	(fu)	+491	+396	(bu)	+945	+1548

[a] The labels min1 and min2 refer to the two minima with ΔE_{min} giving the energy difference between them, E(min2) − E(min1), for the ASP and MP2 calculations. The four single flip and bifurcation transition states are given in the same way with ΔE_{ts1} and ΔE_{ts2} representing the barrier heights with respect to the lowest of min1 or min2. All units are in wavenumbers. [b] With DZP basis set.

TABLE 3: Details of the Eight Rearrangements Which Interconvert the Four Minima in Subset {3}[a]

				single flip			bifurcation		
min1	min2	ΔE_{min}^{asp}	$\Delta E_{min}^{mp2\ b}$	TS	ΔE_{ts1}^{asp}	$\Delta E_{ts1}^{mp2\ b}$	TS	ΔE_{ts2}^{asp}	$\Delta E_{ts2}^{mp2\ b}$
(uu){3}	(ud){3}	−224	−257	(uf)	+366	+187	(ub)	+689	+887
(ud){3}	(dd){3}	+206	+261	(fd)	+354	+293	(bd)	+632	+967
(dd){3}	(du){3}	+234	+295	(df)	+374	+162	(db)	+722	+850
(du){3}	(uu){3}	−216	−299	(fu)	+379	+321	(bu)	+644	+1001

[a] The labels min1 and min2 refer to the two minima with ΔE_{min} giving the energy difference between them, E(min2) − E(min1), for the ASP and MP2 calculations. The four single flip and bifurcation transition states are given in the same way with ΔE_{ts1} and ΔE_{ts2} representing the barrier heights with respect to the lowest of min1 and min2. All units are in wavenumbers. [b] With DZP basis set.

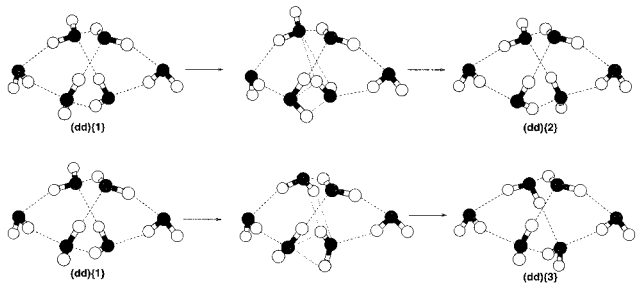

Figure 6. Two of the eight rearrangements which interconvert structures between subsets {1} and {2} (top path) and subsets {1} and {3} (bottom path).

they too may be observed experimentally and the question as to whether they themselves may actually be present in the ground state is considered in section 5. The *ab initio* calculations confirm that the topology of the ASP-W2 surface in the region of the cage is correct but suggest that barriers between minima may be fairly inaccurate.

More transition states were found, all with barriers greater than 1000 cm^{-1} on the ASP-W2 surface, which facilitate interconversion between the {1} and {2} subsets and the {1} and {3} subsets. A given structure can transform into only one of the four in the other subsets having the correct orientation of free hydrogens so eight (2 × 4) and not 32 (2 × 16) transition states exist to facilitate these rearrangements. The two examples of these rearrangements are shown in Figure 6. The other six paths are analogous to those shown, differing only in the positions of the unbound hydrogens. The mechanisms involve motion of two monomers and are similar to the donor−acceptor tunneling in the water dimer.[67] The four dotted lines in the transition state show the two bonds breaking and the two forming, while the dashed lines represent hydrogen bonds which exist in both minimum energy structures. Each transition state shows a bifurcation, as characterized in transitions states in the water trimer[68,69] and water pentamer.[12,70] In addition, there can be seen two water monomers in an arrangement similar to that of the C_2 transition state for donor−acceptor tunneling in the water dimer.[71] This is seen most clearly as the rectangular shape in the transition state in the top path, while the bifurcation is best seen as the triangular arrangement in the transition state of the bottom path. The energetics of the eight rearrangements

TABLE 4: Details of the Eight Rearrangements Which Interconvert Equivalent Structures within the {1}, {2}, and {3} Subsets[a]

min1	min2	ΔE_{min}^{asp}	ΔE_{min}^{MP2}	ΔE_{ts1}^{asp}	$\Delta E_{ts1}^{mp2\ b}$
(uu){1}	(uu){2}	+414	+569	+1236	+1786
(ud){1}	(ud){2}	+200	+315	+1123	+1579
(du){1}	(du){2}	+605	+874	+1160	+1669
(dd){1}	(dd){2}	+407	+629	+1164	+1874
(ud){1}	(ud){3}	+247	+395	+1051	+1577
(dd){1}	(dd){3}	+441	+695	+1151	+1579
(du){1}	(du){3}	+707	+1029	+1215	+2022
(uu){1}	(uu){3}	+537	+721	+1127	+1921

[a] The labels min1 and min2 refer to the two minima with ΔE_{min} giving the energy difference between them, E(min2) − E(min1), for the ASP and MP2 calculations. The four transition states are given in the same way ΔE_{ts} representing the barrier height with respect to min1. All units are in wavenumbers. [b] With DZP basis set.

are outlined in Table 4. The ASP-W2 barriers are consistently lower than the DZP/MP2 barriers, although the agreement is still reasonable.

No transition states corresponding to interconversions between subsets {2} and {3} were found. This could be because the barriers are so high that the structures were not located or simply that they do not exist. In fact, by looking at the {2} and {3} structures in Figure 3, it can be seen that they cannot be interconverted without movement of at least three water monomers, a more complicated mechanism than those shown in Figure 6.

Figure 7 shows relative positions of the 12 minima on the ASP-W2 and DZP/MP2 surfaces (not all the necessary calculations were done for the 6-31G[2d,1p] basis set). Numbers are shown indicating barrier heights for the interconversions between all like types of minima in difference subsets. It can be seen that the ASP-W2 and DZP/MP2 topologies and barriers are in reasonable agreement.

It is therefore possible, in principle at least, to interconvert all of the 12 cage minima characterized here, although interconversion between one of the {2} and {3} subsets would need to go via the corresponding lower energy {1} structure. It would seem unlikely that such interconversions are possible, especially at low temperature, because of the relatively high barriers and energetic displacement of the relative minima. However, this is a question that will be addressed in section 5.

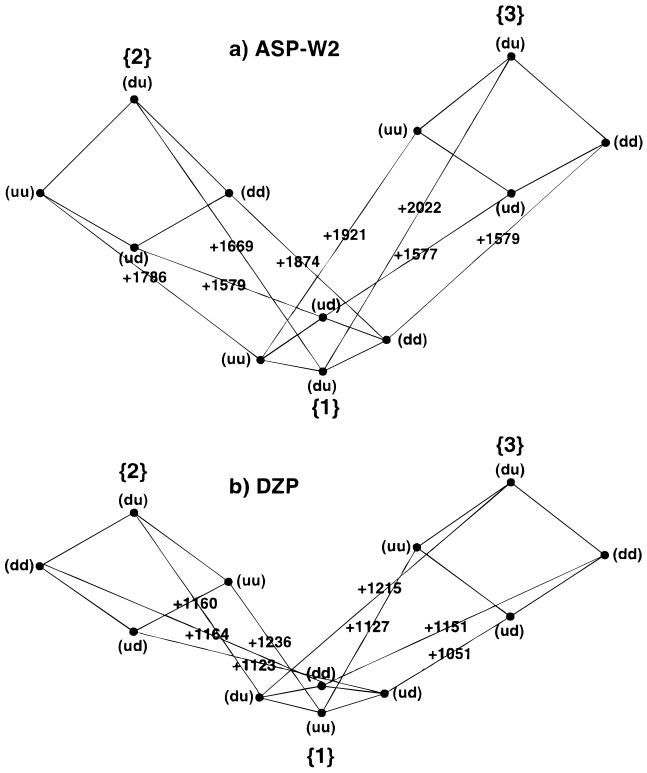

Figure 7. Diagrams showing the arrangement of 12 cagelike minima labeled as subsets {1}, {2}, and {3} for the empirical potential and the DZP/MP2 *ab initio* surface.

TABLE 5: Rotational Constants (MHz) for the Four Most Stable Cage Structures (Subset{1}). Also Shown Are the Vibrationally Averaged RBDMC Values and Experimental Numbers

	{ud}	{uu}	{dd}	{du}	vib av
			DZP		
A	2173	2179	2173	2185	
B	1115	1121	1113	1112	
C	1067	1072	1064	1065	
			6-31G[2d,1p]		
A	2281	2291	2280	2299	
B	1160	1159	1156	1157	
C	1110	1105	1111	1110	
			ASP		
A	2318	2333	2320	2345	2136
B	1198	1195	1190	1195	1096
C	1146	1139	1145	1145	1043
			Experiment		
A					2164
B					1131
C					1069

4. Rotational Constants

Table 5 shows the rotational constants for the four minima in subset {1} compared to the experimental and theoretical values reported previously in ref 30. All four minima have almost identical rotational constants, which is not surprising since structurally they differ only in the positions of two hydrogen atoms. The DZP/MP2 values show good agreement with experiment, whereas the 6-31G[2d,1p] basis set gives values seemingly too high. However, the ASP values are quite close to the 6-31G[2d,1p] values and give good agreement with experiment in the RBDMC simulations of ref 30. This implies that the 6-31G[2d,1p]/MP2 geometries are more accurate than those with the smaller DZP basis set. This also highlights a problem in comparing theory with experiment in that cancellation between the errors caused by the neglect of vibrational averaging, together with those due to finite basis sets and limited inclusion of electron correlation, can lead to accidental good agreement.

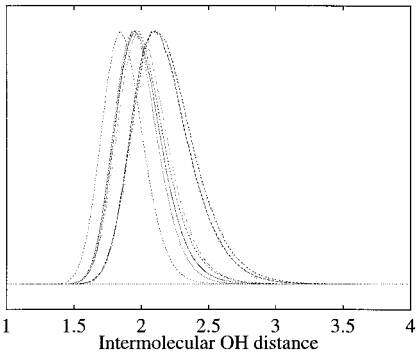

Figure 8. Wave functions for the O···H distances (Å) for the eight hydrogen bonds labeled corresponding to subset {1}.

5. Quantum Simulations

After a thorough characterization of the topology of the potential energy surface of the cage water hexamer is made, the RBDMC method is applied, using the ASP-W2 surface, to simulate the vibrational ground state. This will provide insight into the two questions raised by the characterization of 12 minima and (in total) 32 transition states in the previous section: firstly, is the ground state a superposition of all four low energy minima shown in Figure 2; secondly, is interconversion possible between these (subset {1}) and any of the other eight minima (subsets {2} and {3}).

In the quantum simulation, 250 replicas in the total population of 3000 were given starting coordinates corresponding to each of the 12 minima. To show the character of the ground state structure, the atoms were labeled as in Figure 2 and the corresponding hydrogen bonds wave functions were obtained. Figure 8 shows these wave functions which appear to be localized. Since at least two hydrogen bonds must be broken in order for the cage to rearrange into structures of the type {2} and {3}, the implication of this is that only structures in subset {1} are present. The corresponding vibrationally averaged distances were also calculated and there is quite a variation between the shortest (1.87 Å) and longest (2.19 Å). However, given that the corresponding vibrationally averaged separation in the water dimer is 2.20 Å[13] and that the wave functions all seem to be localized on a single well, there is no evidence that any hydrogen bond exchange motions leading to the higher energy structures in subsets {2} and {3} (or other isomers with different hydrogen bond networks) take place. Although the DZP/MP2 results suggest that the ASP-W2 separation of minima and barrier heights are overestimated, this would probably not be sufficient to alter this conclusion.

To show which of the four minima in Figure 2 contribute to the ground state structure, it is necessary to look at the angles of the hydrogens on the far left and far right of these structures since this is the only way in which they differ. To describe this motion, four internal angles can be defined by taking three midpoints between the two oxygens on the far left and far right (m_1), the two at the top (m_2), and the two at the front (m_3). These three midpoints can be used to define two vectors, $\mathbf{v}_1 = m_2 - m_1$ and $\mathbf{v}_2 = m_3 - m_1$, which are shown in Figure 9. In turn, these vectors can be used to define four angles: θ_{1a}, which is the angle between $\mathbf{v}_1$ and the O−H bond on the far left, θ_{1b}, which is a similar angle defined with $\mathbf{v}_2$, and two more angles, θ_{2a} and θ_{2b}, which are similar but involve the other free hydrogen.

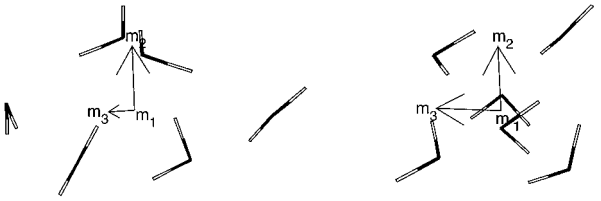

Figure 9. The two vectors used to define the movement of the free hydrogens. Two views are shown.

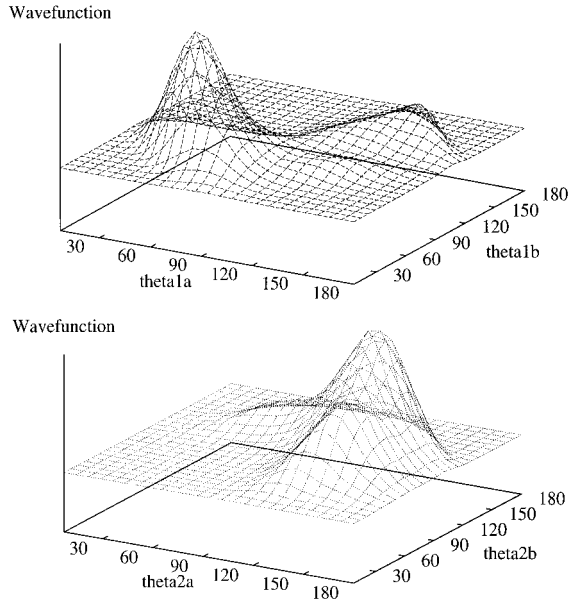

Figure 10. Two-dimensional wave functions for the free hydrogens on the far left and right of the cage structures as shown in Figure 1. The axes are labeled in degrees.

Using the four angles described, two-dimensional wave functions were averaged in the simulation on a 25 × 25 grid with each angle defined between 0° and 180°; these wave functions are shown in Figure 10. The wave function is largely localized on one minimum, that corresponding to the lowest energy (uu) structure. The top wave function does show some delocalization due to the presence of the (du) structure, which has a relative energy of +32 cm^{-1} on the ASP-W2 surface, but the bottom wave function shows none of the delocalization which would arise due to the (dd) and (du) minima in the ground vibrational state. Although the DZP/MP2 *ab initio* results give different ordering of the four minima, their relative energy differences were similar to those for the ASP-W2 surface. However, the DZP/MP2 and to a lesser extent 6-31G[2s,1p]/MP2 barriers for this flipping motion are actually smaller and it is therefore possible that the cage hexamer observed experimentally is actually to some extent a superposition of all four minima in Figure 2. However, the wave function obtained suggested that it is extensively localized on a single minimum. To verify this exactly would require a potential energy surface with barriers and relative energies of these four minima in very close agreement with very accurate *ab initio* calculations.

6. Conclusions

The water hexamer is a hugely challenging system to which to apply theoretical methods. This complexity is a result of the large number of low energy minima on the potential energy surface and the fact that a cyclic conformation is almost certainly not favored.

A closer examination of possibly the most stable hexamer structure, the cage, reveals a more complicated situation still. There are actually four minima, of which the cage structure in Figure 1 is one, which lie within 100 cm^{-1} of one another on the ASP-W2 and DZP/MP2 surfaces. Furthermore, these four structures may interconvert via facile single flips of unbound hydrogens similar to those characterized for the cyclic water trimer[68] and pentamer.[70] The four transition states mediating these near-degenerate rearrangements have barriers between 381 and 510 cm^{-1} on the ASP-W2 surface. Analogous bifurcation mechanisms can mediate the same processes but the barriers are always higher than those for the corresponding single flip. The implication of this is that, even at low temperatures, a superposition of these four structures could possibly be observed.

Two more subsets of four cage structures exist of the ASP-W2, DZP/MP2, and 6-31G[2d,1p]/MP2 surfaces which are only slightly higher in energy than the first four. Again these structures are linked to one another by trivial single flips with low barriers and by bifurcations with higher barriers. The three different subsets may interconvert by means of high-energy rearrangements for which the barriers are all greater than 1000 cm^{-1} on the ASP-W2 surface. The transition states have hydrogen bond arrangements in which monomers adopt orientations similar to two of the transition states in the water dimer.

Quantum simulation of the water hexamer shows no evidence of hydrogen-bond exchange motions evidenced from examination of the eight corresponding wave functions. This implies that the eight higher energy structures of the complex are not present at 0 K. Examination of the wave function for the flipping coordinates of the two single donor−single acceptor water monomers further implies that the ground state is predominantly made up of the lowest energy structure, (du{1}, on the ASP-W2 surface. However, the relevant barriers obtained with the best *ab initio* calculations, 6-31G[2d,1p]/MP2, are smaller than those on the ASP-W2 surface. This suggests that there could be more delocalization of the ground state wave function on other structures.

The water hexamer observed experimentally[30] is probably largely based upon a single minimum. This structure is probably the (du){1} isomer shown in Figure 2 since both sets of *ab initio* calculations suggest it to be lowest in energy. A slight delocalization on some or all of the other three structures in Figure 2 is likely, probably more than is suggested by the highly localized wave functions shown in Figure 10 which are calculated with the ASP-W2 surface, for which the corresponding barriers and relative separation of minima are too large. It is, however, very unlikely that any of the other eight minima would be present at the low temperatures (<10 K) of supersonic beams.

Recent FIR-VRT experiments have observed tunneling fine structure in the water hexamer spectrum.[72] These have been rationalized in terms of a degenerate tunneling process. Such a process would not correspond to any of the rearrangement reported here. However, we have identified two degenerate rearrangements (out of several hundred in total) involving the double donor−single acceptor monomers. We are currently calculated the tunneling pattern arising from these rearrangements.[73]

This study emphasizes that more accurate *ab initio* calculations are required to provide an accurate description of the energetics of the structures and transition states characterized here. The formulation of a 30-dimensional potential energy surface (ASP-W2), which agrees fairly well with quite accurate *ab initio* calculations but is simple enough to use in quantum simulations where many discrete points are required, is very useful. However, there is now needed an even more accurate

surface which can reproduce the minima and transition states calculated using the most accurate *ab initio* methods.

Two points of general relevance to the study of water clusters are worthy of emphasis in the present work: first, that a quite complicated water hexamer rearrangement goes via a transition state in which the three monomers in the process of moving adopt arrangements resembling transition states in the water dimer (Figure 6); second, the fact that a floppy cluster, which has of the order of hundreds of minima accessible to the ground state, could be localized on just one. It is these general observations, as well as accurate theoretical calculations, that help in moving toward a more detailed understanding of bulk water.

Acknowledgment. J.K.G. is grateful to Richard Saykally and David Wales for useful discussions and to Anthony Stone for making available the ORIENT 3 program and ASP-W2 data.

References and Notes

(1) Dyke, T. R.; Mack, K. M.; Muenter, J. S. *J. Chem. Phys.* **1977**, *66*, 498.
(2) Scheiner, S. *Annu. Rev. Phys. Chem.* **1994**, *45*, 23.
(3) Loeser, J. G.; Schuttenmaer, C. A.; Cohen, R. C.; Elrod, M. J.; Steyery, D. W.; Saykally, R. J.; Bumgarner, R. E.; Blake, G. A. *J. Chem. Phys.* **1992**, *97*, 4727.
(4) Cohen, R. C.; Saykally, R. J. *J. Phys. Chem.* **1992**, *96*, 1024.
(5) Elrod, M. J.; Saykally, R. J. *Chem. Rev.* **1994**, *94*, 1975.
(6) Xantheas, S. S. *J. Chem. Phys.* **1994**, *100*, 7523.
(7) Xantheas, S. S. *J. Chem. Phys.* **1995**, *102*, 4505.
(8) Tsai, C. J.; Jordan, K. D. *Chem. Phys. Lett.* **1993**, *213*, 181.
(9) Kim, K.; Jordan, K. D.; Zwier, T. S. *J. Am. Chem. Soc.* **1994**, *115*, 11568.
(10) Gregory, J. K.; Clary, D. C. *J. Chem. Phys.* **1995**, *102*, 7817.
(11) Gregory, J. K.; Clary, D. C. *J. Chem. Phys.* **1995**, *103*, 8924.
(12) Gregory, J. K.; Clary, D. C. *J. Chem. Phys.* **1996**, *105*, 6626.
(13) Gregory, J. K.; Clary, D. C. *J. Phys. Chem.* **1996**, *100*, 18014.
(14) Gregory, J. K.; Clary, D. C.; Liu, K.; Brown, M. G.; Saykally, R. J. *Science* **1997**, *275*, 814.
(15) Liu, K.; Elrod, M. J.; Loeser, J. G.; Cruzan, J. D.; Pugliano, N.; Brown, M. G.; Rzepiela, J. A.; Saykally, R. J. *Faraday Discuss.* **1994**, *97*, 35.
(16) Pugliano, N.; Saykally, R. J. *Science* **1992**, *257*, 1937.
(17) Liu, K.; Loeser, J. G.; Elrod, M. J.; Host, B. C.; Rzepiela, J. A.; Pugliano, N.; Saykally, R. J. *J. Am. Chem. Soc.* **1994**, *116*, 3507.
(18) Bene, J. E. Del; Pople, J. A. *J. Chem. Phys.* **1973**, *58*, 3605.
(19) Fowler, J. E.; Schaefer, H. F. *J. Am. Chem. Soc.* **1995**, *117*, 446.
(20) Kim, K. S.; Dupuis, M.; Clementi, E. *Chem. Phys. Lett.* **1986**, *131*, 451.
(21) Cruzan, J. D.; Braly, L. B.; Liu, K.; Brown, M. G.; Loeser, J. G.; Saykally, R. J. *Science* **1996**, *271*, 59.
(22) Cruzan, J. D.; Brown, M. G.; Liu, K.; Braly, L. B.; Saykally, R. J. **1996**, *105*, 6634.
(23) Honegger, E.; Leutwyler, S. *J. Chem. Phys.* **1988**, *88*, 2582.
(24) Xantheas, S. S., Jr.; Dunning, T. H. *J. Chem. Phys.* **1993**, *98*, 8037.
(25) Xantheas, S. S.; Dunning, T. H. *J. Chem. Phys.* **1993**, *99*, 8774.
(26) Liu, K.; Brown, M. G.; Cruzan, J. D.; Saykally, R. J. *Science* **1996**, *271*, 62.
(27) Knochenmuss, R.; Leutwyler, S. *J. Chem. Phys.* **1992**, *96*, 5233.
(28) Tsai, C. J.; Jordan, K. D. *J. Chem. Phys.* **1991**, *95*, 3850.
(29) Saykally, R. J.; Blake, G. A. *Science* **1993**, *259*, 1570.
(30) Liu, K.; Brown, M. G.; Saykally, R. J.; Gregory, J. K.; Clary, D. C. *Nature* **1996**, *391*, 501.
(31) Mhin, B. J.; Kim, J.; Lee, S.; Lee, J. Y.; Kim, K. S. *J. Chem. Phys.* **1994**, *100*, 4484.
(32) Franken, K. A.; Jalaie, M.; Dykstra, C. E. *Chem. Phys. Lett.* **1992**, *198*, 59.
(33) Schröder, F. H. *Chem. Phys.* **1988**, *123*, 91.
(34) Vegiri, A.; Farantos, S. C. *J. Chem. Phys.* **1993**, *98*, 4059.
(35) Mhin, B. J.; Kim, H. S.; Kim, H. S.; Yoon, C. W.; Kim, K. S. *Chem. Phys. Lett.* **1991**, *176*, 41.
(36) Laasonen, K.; Parrinello, M.; Car, R.; Lee, C.; Vanderbilt, D. *Chem. Phys. Lett.* **1993**, *207*, 208.
(37) Lee, C.; Chen, H.; Fitzgerald, G. *J. Chem. Phys.* **1994**, *101*, 4472.
(38) Belford, D.; Campbell, E. S. *J. Chem. Phys.* **1987**, *86*, 7013.
(39) Tsai, C. J.; Jordan, K. D. *J. Phys. Chem.* **1993**, *97*, 5208.
(40) Millot, C.; Stone, A. J. *Mol. Phys.* **1992**, *77*, 439.
(41) Millot, C.; Soetens, J. C.; Costa, M. T. C.; Martins; Hodges, M.; Stone, A. J. Preprint.
(42) Popelier, P. L. A.; Stone, A. J.; Wales, D. J. *Faraday Discuss. Chem. Soc.* **1994**, *97*, 243.
(43) Wales, D. J.; Stone, A. J.; Popelier, P. L. A. *J. Chem. Phys.* **1995**, *102*, 5551.
(44) Wales, D. J.; Stone, A. J.; Popelier, P. L. A. *Chem. Phys. Lett.* **1995**, *240*, 89.
(45) Stone, A. J. *Chem. Phys. Lett.* **1981**, *83*, 233.
(46) Alderton, M.; Stone, A. J. *Mol. Phys.* **1985**, *56*, 1047.
(47) Popelier, P. L. A.; Stone, A. J. *Mol. Phys.* **1994**, *82*, 411.
(48) Cerjan, C. J.; Miller, W. H. *J. Chem. Phys.* **1981**, *75*, 2800.
(49) Amos, R. D. *CADPAC: Cambridge Analytical Derivatives Package (Version 5)*; University of Cambridge: Cambridge, U.K., 1992.
(50) Møller, C.; Plesset, M. S. *Phys. Rev.* **1934**, *46*, 618.
(51) Dunning, T. H. *J. Chem. Phys.* **1970**, *53*, 2823.
(52) Fredericks, S. Y.; Jordan, K. D.; Zwier, T. S. *J. Phys. Chem.* **1996**, *100*, 7810.
(53) Kendall, R. A.; Dunning, T. H.; Harrison, R. J. *J. Chem. Phys.* **1992**, *96*, 6796.
(54) Anderson, J. B. *J. Chem. Phys.* **1975**, *63*, 1499.
(55) Anderson, J. B. *Int. Rev. Phys. Chem.* **1995**, *14*, 85.
(56) Coker, D. F.; Watts, R. O. *Mol. Phys.* **1986**, *58*, 1113.
(57) Miller, R. E.; Coker, D. F.; Watts, R. O. *J. Chem. Phys.* **1985**, *82*, 3554.
(58) Coker, D. F.; Watts, R. O. *J. Phys. Chem.* **1987**, *91*, 2513.
(59) Sun, H.; Watts, R. O. *J. Chem. Phys.* **1990**, *92*, 603.
(60) Quack, M.; Suhm, M. A. *J. Chem. Phys.* **1991**, *95*, 28.
(61) Lewerenz, M.; Watts, R. O. *Mol. Phys.* **1994**, *81*, 1075.
(62) Gregory, J. K.; Clary, D. C. *Chem. Phys. Lett.* **1994**, *228*, 547.
(63) Reimers, J. R.; Watts, R. O. *J. Chem. Phys.* **1984**, *85*, 83.
(64) Suhm, M. A.; Watts, R. O. *Phys. Rep.* **1991**, *204*, 293.
(65) Gregory, J. K. To be published.
(66) Kalos, M. H. *Phys. Rev. A* **1967**, *2*, 250.
(67) Coudert, L. H.; Hougen, J. T. *J. Mol. Spectrosc.* **1990**, *139*, 259.
(68) Wales, D. J. *J. Am. Chem. Soc.* **1993**, *115*, 11180.
(69) Walsh, T. R.; Wales, D. J. *J. Chem. Soc., Faraday Trans.* **1996**, *92*, 2505.
(70) Wales, D. J.; Walsh, T. R. *J. Chem. Phys.* **1996**, *105*, 6957.
(71) Smith, B. J.; Swanton, D. J.; Pople, J. A.; Schaefer, H. F.; Radom, L. *J. Chem. Phys.* **1990**, *92*, 1240.
(72) Saykally, R. J. Private communication.
(73) Gregory, J. K. To be published.